Characterization of Canine Osteosarcoma by Array Comparative Genomic Hybridization and RT-qPCR: Signatures of Genomic Imbalance in Canine Osteosarcoma Parallel the Human Counterpart

Andrea Y. Angstadt,[1] Alison Motsinger-Reif,[2,3,4] Rachael Thomas,[1,2] William C. Kisseberth,[5,6] C. Guillermo Couto,[5,6] Dawn L. Duval,[7] Dahlia M. Nielsen,[3,8] Jaime F. Modiano,[9,10] and Matthew Breen[1,2,11]*

[1]Department of Molecular Biomedical Sciences, North Carolina State University, Raleigh, NC
[2]Center for Comparative Medicine and Translational Research, North Carolina State University, Raleigh, NC
[3]Bioinformatics Research Center, North Carolina State University, Raleigh, NC
[4]Department of Statistics, North Carolina State University, Raleigh, NC
[5]Department of Veterinary Clinical Sciences, College of Veterinary Medicine, The Ohio State University, Columbus, OH
[6]Comprehensive Cancer Center and Solove Research Institute, The Ohio State University, Columbus, OH
[7]Department of Clinical Sciences, Animal Cancer Center, Colorado State University, Fort Collins, CO
[8]Department of Genetics, North Carolina State University, Raleigh, NC
[9]Masonic Cancer Center, University of Minnesota, Minneapolis, MN
[10]Department of Veterinary Clinical Sciences, College of Veterinary Medicine, University of Minnesota, St. Paul, MN
[11]Cancer Genetics Program, UNC Lineberger Comprehensive Cancer Center, Chapel Hill, NC, USA

Osteosarcoma (OS) is the most commonly diagnosed malignant bone tumor in humans and dogs, characterized in both species by extremely complex karyotypes exhibiting high frequencies of genomic imbalance. Evaluation of genomic signatures in human OS using array comparative genomic hybridization (aCGH) has assisted in uncovering genetic mechanisms that result in disease phenotype. Previous low-resolution (10–20 Mb) aCGH analysis of canine OS identified a wide range of recurrent DNA copy number aberrations, indicating extensive genomic instability. In this study, we profiled 123 canine OS tumors by 1 Mb-resolution aCGH to generate a dataset for direct comparison with current data for human OS, concluding that several high frequency aberrations in canine and human OS are orthologous. To ensure complete coverage of gene annotation, we identified the human refseq genes that map to these orthologous aberrant dog regions and found several candidate genes warranting evaluation for OS involvement. Specifically, subsequent FISH and qRT-PCR analysis of RUNX2, TUSC3, and PTEN indicated that expression levels correlated with genomic copy number status, showcasing RUNX2 as an OS associated gene and TUSC3 as a possible tumor suppressor candidate. Together these data demonstrate the ability of genomic comparative oncology to identify genetic abberations which may be important for OS progression. Large scale screening of genomic imbalance in canine OS further validates the use of the dog as a suitable model for human cancers, supporting the idea that dysregulation discovered in canine cancers will provide an avenue for complementary study in human counterparts. © 2011 Wiley-Liss, Inc.

INTRODUCTION

Osteosarcoma (OS) is the most commonly diagnosed primary malignant tumor of the bone in humans (Withrow and Vail, 2007; Mirabello et al., 2009a,b), with fewer than 1,000 new diagnoses per year in the USA (Mirabello et al., 2009b; Paoloni et al., 2009). The introduction of chemotherapy regimens in the 1980's, including treatment before and after definitive surgical resection, helped to improve the five-year survival rate to ∼ 70%, but little improvement to this rate has been made in the last decade. Better understanding of the biological mechanisms driving this aggressive malignancy requires a detailed knowledge of the underlying genomic changes associated with tumor

initiation and progression. Molecular cytogenetic evaluation of human OS, using a combination of comparative genomic hybridization (CGH), spectral karyotyping (SKY), and multicolor banding (mBAND) has identified extensive and frequent genome reorganization. Such reorganization includes a high degree of aneuploidy, gene amplification, and multiple unbalanced chromosomal rearrangements (Bridge et al., 1997; Bayani et al., 2003; Ozaki et al., 2003; Lim et al., 2004; Man et al., 2004) Analysis of human OS by array comparative genomic hybridization (aCGH) has revealed high amplitude copy number gain ($\log_2$ ratio of tumor:reference ≥ 1.0) or amplification ($\log_2$ ratio of tumor:reference ≥ 2.0) to be frequent events in human OS, particularly within the cytogenetic regions defined by 6p22-p21, 8q24 and 17p12-p11.2 (Forus et al., 1995; Tarkkanen et al., 1995, 1998, 1999; Simons et al., 1997; Zielenska et al., 2001; Bayani et al., 2003; Squire et al., 2003; Selvarajah et al., 2008). The frequency of occurrence of recurrent genomic amplifications suggests that they may harbor genes important in tumorigenesis and/or tumor progression (Lu et al., 2008; Sadikovic et al., 2009). Recent studies in human OS have reported strong associations between gene copy number aberration, overexpression, and hypomethylation leading to disease progression (Sadikovic et al., 2009).

The complexity of human OS karyotypes (Papachristou and Papavassiliou, 2007; Clark et al., 2008; Tang et al., 2008) combined with the rarity of the disease, impedes the ability to define specific genetic changes that ultimately may lead to the disease phenotype. Pathogenetic knowledge gained from analysis of model organisms is a key complimentary approach to advance gene discovery. In the domestic dog, OS also is the most common primary bone tumor (Withrow and Vail 2007), but in contrast to the occurrence in humans, the annual number of new cases of canine OS (in the US) is estimated to far exceed 10,000 (Withrow et al., 1991; Fossey et al., 2009). The spontaneous nature and high frequency of occurrence in dogs thus provides a unique opportunity to evaluate the extent of aberrant genomic events in canine OS, knowledge of which will highlight key regions of shared pathogenesis and may reveal additional regions as yet unidentified in human OS. Until recently, very few studies in canine OS have profiled genomic instability, largely because of the paucity of resources for canine genomic studies. The release of the annotated canine genome assembly (Lindblad-Toh

et al., 2005) facilitated the development of genome integrated molecular cytogenetic reagents for the dog (Thomas et al., 2005, 2007, 2008), allowing more comprehensive cytogenetic studies to be performed. In an earlier study we used low-resolution (10–20 Mb) aCGH analysis of 38 cases of canine OS to identify a high degree of gross genomic instability, with extensive cytogenetic disorganization consistent with those observed in human OS (Thomas et al., 2009b, 2011). In addition, several previous studies have sought to define the roles of specific tumor suppressor genes and oncogenes, both in primary canine OS and canine OS cell lines, using expression and proteomic analysis (Levine and Fleischli, 2000; Levine, 2002; Kirpensteijn et al., 2008; Fossey et al., 2009; Zhang et al., 2009). Genomic disorganization in OS of both species has been reported to involve the dysregulation of well known tumor suppressor genes (*TP53*, *RB1*, *PTEN*, *CDKN2A*, *CDKN2B*) and oncogenes (*MYC* and *MET*) (Feugeas et al., 1996; Levine and Fleischli, 2000; Tsuchiya et al., 2000; Gokgoz et al., 2001; Levine et al., 2002; Overholtzer et al., 2003; Kirpensteijn et al., 2008; De Maria et al., 2009; Zhang et al., 2009).

While the human and canine autosomal genomes are packaged into 22 and 38 chromosomes, respectively, comparative genomics indicates that we may regard the two species as sharing 200+ evolutionarily conserved genomic regions (Derrien et al., 2007). By examining recurrent cytogenetic aberrations in human and canine cancers at a higher resolution, this comparative approach already has been shown to substantially improve the ability to pinpoint the shared aberrant regions to defined smaller subregions, thereby providing an accelerated path to gene discovery (Thomas et al., 2009b, 2011). In this current study, we profiled 123 cases of canine OS using genome-integrated 1 Mb-resolution aCGH to further identify recurrent cytogenetic changes at a resolution suitable for direct comparison with data currently available for human OS. The cohort analyzed in this study comprised four target breeds of dog, each of which exhibits a high occurrence of OS: Golden Retriever, Great Pyrenees, retired racing Greyhound, and Rottweiler, as well as individuals from a variety of other breeds collectively described as a 'non-target' breed group. We identified recurrent high frequency DNA copy number aberrations (CNAs) within our sample set that are orthologous to regions of recurrent genome imbalance identified

TABLE 1. Summary of Breed and Morphological Subtype of 123 Canine OS Tumor Samples Analyzed for DNA Copy Number Aberrations by Genome Integrated 1Mb-Resolution aCGH

Breed	Total cases	OS subtype			
		Chondroblastic	Fibroblastic	Osteoblastic	Undetermined
American Bulldog	1			1	
Bernese Mountain Dog	1				1
Borzoi	1			1	
Boxer	1		1		
Briard	1				1
Collie	1				1
Doberman	4		1	3	
Flat Coat Retriever	2				2
German Shepherd	1			1	
Golden Retriever	22	3	1	13	5
Great Dane	2	1	1		
Great Pyrenees	13	3	2	4	4
Greyhound	25	1	1	16	7
Irish Setter	2			2	
Labrador Retriever	3			1	2
Mastiff	2			1	1
Mix	4			1	3
Rhodesian Ridgeback	2			1	1
Rottweiler	34	4	6	21	3
Saint Bernard	1			1	
Total	*123*	*12*	*13*	*67*	*31*

A detailed list of all cases is provided in Supporting Information Table 1.

in human OS and observed also that genomic instability in canine OS is associated with morphological subtypes (osteoblastic, chondroblastic, and fibroblastic). To evaluate the effect of genomic CNA on gene expression, quantitative real time polymerase chain reaction (qRT-PCR) analysis of a targeted set of genes was performed on 26 canine OS samples.

MATERIALS AND METHODS

Tissue Specimens

Canine OS tissues were collected from cases of spontaneously occurring canine OS by institutional or community veterinary practices in the United States between November 1999 and July 2009. A total of 123 canine OS tumor specimens (Table 1 and Supporting Information Table 1) were obtained with informed consent of the owners and during routine clinical evaluation prior to the initiation of chemotherapy or radiotherapy. Tissue specimens were processed as described previously (Thomas et al., 2005). Briefly, tumor tissue was surgically removed under sterile conditions as a part of a diagnostic biopsy procedure and grossly normal tissue was excised from the specimen. Tumor tissue was then (1) fixed in formalin and submitted for histological evaluation of

hematoxylin and eosin (H&E)-stained sections, using the criteria of Kirpensteijn et al (Kirpensteijn et al., 2002), (2) processed immediately for DNA extraction, and (3) used to initiate primary cell cultures in RPMI-1640 (Mediatech, Manassas, VA) medium supplemented with 10% fetal bovine serum (Mediatech, Manassas, VA, 2mM L-glutamine (Mediatech, Manassas, VA) and 100 µg/ml Primocin (Invivogen, San Diego, CA).

Array Comparative Genomic Hybridization (aCGH)

A genomic microarray comprising cytogenetically-mapped bacterial artificial chromosome (BAC) clones was used for array CGH analysis. Clones used for this array (all from the CHORI-82 dog BAC library—http://bacpac.chori.org, BACPAC Resources, Children's Hospital Oakland Research Institute, Oakland, CA) were distributed at ∼ 1 Mb intervals throughout each dog autosome and the X chromosome, and was supplemented with additional clones representing cancer related genes (Thomas et al., 2008, 2009a). To minimize opportunities for generating data representing naturally occurring copy number variants not associated with OS, reference DNA samples used in this study were derived either from the patient's own blood (where

available) or from equimolar pools of DNA from ≥10 cancer free, healthy, sex-mismatched dogs of the same breed. Conventional phenol:chloroform extraction was used to isolate high molecular weight DNA from both tumor and reference samples. Tumor (test) and reference DNA samples were differentially labeled with Cyanine-3-dCTP and Cyanine-5-dCTP, respectively and then combined in the presence of dog C_ot_1 DNA as competitor. The probe mixture was denatured and applied to the microarray for 40 hr at 37°C as described previously (Thomas et al., 2007). Following post hybridization, stringency washes the arrays were scanned at 10 μm resolution (Perkin Elmer ScanArray Express). The fluorescence intensity at each genomic locus was quantified and used to calculate the $\log_2$ ratio of test:reference DNA for each locus on the array. Threshold limits for CNAs were set at $\log_2$ ratio (test:reference) values equivalent to 1.15:1 (copy number gain) and 0.85:1 (copy number loss), and the data analyzed by the aCGH Smooth algorithm (Jong et al., 2003). Briefly, the aCGH Smooth algorithm uses a clustering-based approach to identify homogenous groups of probes that define regions of gain or loss. The thresholds selected were used to discretize the $\log_2$ ratio data from all 123 canine OS aCGH data sets and the ratios were converted to ordinal data (loss, normal, gain), which were then evaluated for disease association. For each autosomal locus on the array, the frequency of CNA within the cohort was calculated. All 123 cases were analyzed for inflection points in regions of chromosomal gain, loss, or normal copy number across cases, thus collapsing the data into larger regions of contiguous copy number status. To make direct comparisons of the genomic imbalance shared between human and dog, orthologous regions of human chromosomal segments defined previously to have a high rate of aneuploidy in OS were identified in the canine genome using the UCSC Genome Browser (http://genome.ucsc.edu/) and Autograph tool (Derrien et al., 2007). Chromosomal locations are defined in terms of their megabase position within the 7.5x dog genome sequence assembly (canFam2.0 May 2005, Lindblad-Toh et al, 2005) according to the UCSC Genome Browser. To ensure complete gene annotation coverage of recurrent regions of aberration in our dog OS cohort, human refseq genes from the GRCh37/Hg19 build (Feb. 2009), which map to orthologous dog genomic regions, were identified by the UCSC genome table browser. Briefly, the dog

genomic regions based upon base pair positions between BAC sequence positions identified by the UCSC genome table browser in Febuary 2011 were then imported in the table browser. The orthologous human refseq gene IDs which mapped to these regions in the dog genome were then identified according to information stored in the table browser gene and gene predication tracks group. In addition, the identified human refseq gene IDs were then inputted back into the table browser to ensure that the IDs mapped to the correct dog genomic positions. These gene lists were submitted to the Database for Annotation, Visualization, and Integrated Discovery (DAVID) v6.7 for functional annotation analysis (http://david.abcc.ncifcrf.gov/). DAVID maps a large number of interesting genes in a list to the associated biological annotation (e.g. gene ontology terms) and then statistically highlights the most overrepresented (enriched) biological annotation out of thousands of linked terms and contents using advanced modular enrichment algorithims (Huang da et al., 2007).

Single Locus Probe (SLP) Fluorescence *In-Situ* Hybridization (FISH)

Where fresh OS tumor tissue was available, primary cell cultures were initiated using the same biopsy specimen that was used for DNA isolation. Metaphase chromosome preparations and interphase nuclei were produced either directly from the primary tumor tissue or from low passage ($n = 3$) primary cultures using conventional techniques of colcemid arrest, hypotonic treatment, and methanol-glacial acetic acid fixation (Breen et al., 1999). Where viable tumor tissue was not available, tumor cells were isolated from formalin-fixed, paraffin-embedded (FFPE) tumor biopsies and used for interphase FISH analysis. Briefly, 25-μm tissue sections were deparaffinized with xylene prior to immersion in 100% ethanol. Specimens were rinsed, air dried, and immersed in a pepsin solution (750 units/ml in 0.01 N HCl) at 37°C for 20 min then soaked in 1× PBS at 4°C for 48 hr and fixed as a cell suspension in 3:1 methanol-glacial acetic acid. Cell suspensions were dropped onto clean glass slides and air-dried. Multicolor single locus probe (SLP) FISH analysis was then performed to evaluate the distribution of selected copy number changes identified by the aCGH data. BAC clones used as SLPs were selected from within chromosomal regions displaying a range of both normal and

TABLE 2. Primer Sequence of Genes Analyzed by qRT-PCR Analysis of Canine OS RNA

Accession Number	Gene	Location	Sense primer (5′-3′)	Antisense primer (5′-3′)
XM_859874.1	TSC2	Chr6q22:41.90-41.94Mb	TCGTCGGACATCAACAACAT	CCGCAGAGTCCGTGTTAGAT
XM_540336.2	RHOC	Chr9q11.2:3.294-3.329Mb	CATCGACAGCCCCGACAGCC	GCACGGGCTCCTGCTTCATCT
XM_532158.2	RUNX2	Chr12q13:16.73-16.84Mb	TCACTCCACCACCCCGCTGT	TGAAGCACCTGCCTGGCTCT
NM_001003246.1	MYC	Chr13q13:28.23-28.24Mb	TCGCCTATTTGGGAAGACAC	AAGCTGACGTTGAGAGGCAT
XM_844352.1	TUSC3	Chr16q23:41.82-42.04Mb	GCCTAGTGGGATT AGGCCTGGTGG	AGTGCCATGGTCCAA ATCACATCTTC
NM_001003192.1	PTEN	Chr26q25:40.92-40.98Mb	ACTTTGAGTTCCCTCAGCCA	AGGTTTCCTCTGGTCCTGGT
XM_849238.1	C12orf43	Chr26q21:19.85-19.86Mb	GCCTGGGGCTTGGAGCAGTG	TGGGCTCGGAATTCGGGGGT

aberrant copy number changes. These clones were differentially labeled and used in multicolor FISH analysis as described previously (Breen et al., 2004).

The copy number status of six candidate mapped human refseq genes (*MYC*, *PTEN*, *RHOC*, *RUNX2*, *TSC2* and *TUSC3*) located within regions of recurrent genomic imbalance and/or possible cancer-related function, including cell proliferation, transformation, and/or apoptosis identified by DAVID analysis (http://david. abcc.ncifcrf.gov/) (Supporting Information Tables 2, 3, and 4) were assessed by archival multicolor SLP FISH. To increase the size of the FISH signal for assessment of archival specimens a panel of six probe pools was developed where each pool comprised overlapping BAC clones selected using the UCSC genome browser (http:// genome.ucsc.edu). Metaphase preparations from clinically healthy dogs were used to confirm that all six BAC contig probes used for FISH exhibited the expected copy number in non-neoplastic cells ($n = 2$ for autosomal loci). Images from a minimum of 30 cells were used to evaluate the copy number status of each probe in control cells and OS cases. Due to the increased depth of field of fixed nuclei, images were acquired using incremental capture within the SmartCapture 3 program (Digital Scientific Ltd, Cambridge, UK) to accurately record and quantify signals in different focal planes.

Quantitative RT-PCR

A subset of the sample population ($n = 26$) containing copy number aberrations involving the same six candidate genes (*MYC*, *PTEN*, *RHOC*, *RUNX2*, *TSC2* and *TUSC3*) was selected for evaluation using RT-PCR. Snap frozen bone tumor biopsies of these 26 cases were ground with a mortar and pestle in the presence of liquid nitrogen and processed for RNA extraction using the Qiagen RNeasy Mini Kit (Qiagen) according to the manufacturer's instructions. The quality and quantity of RNA was assessed using spectrophotometry (Nanodrop 1000, Nanodrop Technologies) and a RNA 6000 Nano Labchip on the Agilent 2100 Bioanalyzer (Agilent). Total RNA with RNA integrity number > 7 was treated for residual genomic DNA (TURBO DNA-free Kit, Ambion) and 1 µg was reverse transcribed into cDNA (Quantitect Reverse Transcription Kit, Qiagen). Quantitative real-time PCR (qRT-PCR) using the QuantiFast SYBR Green Kit (Qiagen) and an iCycler (BioRad) was performed to evaluate the transcriptional status of the same six genes (evaluated also by SLP FISH analysis. Primers were designed using primer blast (http://www.ncbi.nlm.nih.gov/tools/ primer-blast/) to ensure each sequence was specific for the gene of interest within the dog genome (Table 2). The reaction efficiency for all primers was calculated using serial dilutions of cDNA isolated from non-neoplastic dog femurs from an adult mixed breed, and only primer pairs with efficiencies ranging from 95%–105% were used in subsequent analysis. Relative quantification was performed as described elsewhere (Pfaffl, 2001) using *c12orf43/LOC61155* as the reference gene, selected on the basis of having both normal copy number in >97% of canine OS sample evaluated by aCGH, and a stable expression pattern in qRT-PCR evaluation of 11 canine osteosarcoma samples (Supporting Information Table 5) and 10 nonneoplastic samples (Tsai et al, submitted). We expressed the relative mRNA levels in the tumors as $-\Delta\Delta CT$, where ΔCT is difference in the threshold PCR cycle (*Ct*) value of mRNA of our gene of interest and the corresponding control (*c12orf43/LOC61155*) in each reaction compared with the non-neoplastic dog femur RNA. Fold change was then calculated using the primer efficiencies and $-\Delta\Delta CT$.

Statistical Analysis

Of the 123 cases analyzed by aCGH, 99 cases were associated with survival data, defined as the time period from the date of diagnosis until death by euthanasia. Patients still alive at time of analysis, or deceased from causes other than their OS, were censored. The Kaplan-Meier method was used to generate survival curves, and tests of nonparametric proportional hazards were used to assess significance between the groups in question for the different tests. For quantitative variables, the variables were directly modeled with proportional hazards regression, and for categorical variables, dummy encoding was used, with the most common category used as the reference.

Association analyses were performed with Fisher's exact tests to correlate aberration frequencies with the five breed groups in the OS dataset: Golden Retriever, Great Pyrenees, Greyhound, Rottweiler, and the nontarget breed group. Fisher's exact tests also were used to associate aberration frequencies within the three cellular morphological subtypes of OS evaluated within the present study: osteoblastic, chondroblastic, and fibroblastic. To control family-wise error rates and correct for the multiple comparisons performed, a Bonferroni correction was performed to derive empirically P-value cut-offs of significance that correspond to a family-wise error rate of 0.05 (Abdi, 2007). The correlation between aberration region size and percentages of CNAs was tested by linear regression. A nonparametric Kruskal-Wallis test was performed to evaluate the differences between groups in our qRT-PCR data. Statistical analyses of the data were performed in JMP Genomics v4 and SAS 9.1.3 (SAS Institute).

RESULTS

Clinical Assessment

A total of 123 cases of canine OS (Table 1 and Supporting Information Table 1) were profiled within this study, of which 93 presented with full histomorphological information. As expected from a random sampling of canine OS the majority presented as the osteoblastic (73%) subtype (Table 1), while the remainder comprised approximately equal proportions of fibroblastic (14%) and chondroblastic (13%) OS. Of the dogs in this study, with defined tumor location ($n = 73$), 63% and 37% had OS in the front (proximal) and rear (distal) limbs, respectively. The most common

anatomical location for the tumors was in the appendicular skeleton (radius 35%, humerus 27%, tibia 25%, femur 12%, ulna 0.03%) with one patient having the disease in the maxilla (Supporting Information Table 1). Though a total of 19 breeds were included in our study population, we specifically targeted four breeds that accounted for 76% (94/123) of the cases: retired racing Greyhound ($n = 25$), Great Pyrenees ($n = 13$), Golden Retriever ($n = 22$), and Rottweiler ($n = 34$) (Table 1). The remaining 29 cases (including mixed-breed dogs) with < 5 dogs represented per breed were categorized into a fifth, 'non-target' breed group because of sparsity concerns for the statistical analysis (Peduzzi et al., 1996). No selection was performed for any other clinical characteristics, so the sample should represent a stratified random sample (thus a simple random sample in regards to other variables for each strata, where each breed group represents a strata).

Survival time (measured in weeks from the date of diagnosis to the date of death) and detailed treatment information (Supporting Information Table 1) was available for 99 and 79 dogs respectively, in the study. The latter 79 cases were grouped into three categories representing those that received amputation of the affected limb in combination with chemotherapy ($n = 56$), amputation alone ($n = 15$), and palliative (pain management and radiotherapy) care only ($n = 8$). All clinical covariates were tested for statistically significant relevance to survival time. The breed ($P = 0.7982$), gender ($P = 0.5747$), tumor location ($P = 0.8306$), and morphological subtype ($P = 0.2969$) were not shown to have a statistically significant effect on survival time. As expected, treatment type received by each dog did reveal a statistically significant effect on survival time, demonstrated by a nonparametric proportional hazards test $P = 0.0004$ (Supporting Information Fig. 1). The hazards ratio and confidence intervals are found in Supporting Information Table 6. As expected, these data indicated that amputation in combination with chemotherapy corresponded to longer survival time than dogs which only received chemotherapy treatment without amputation of the affected area.

Abundant Genomic Instability in Canine OS

Individual cases within the canine OS cohort used in this study typically presented with highly complex aCGH profiles, with aberrations ranging
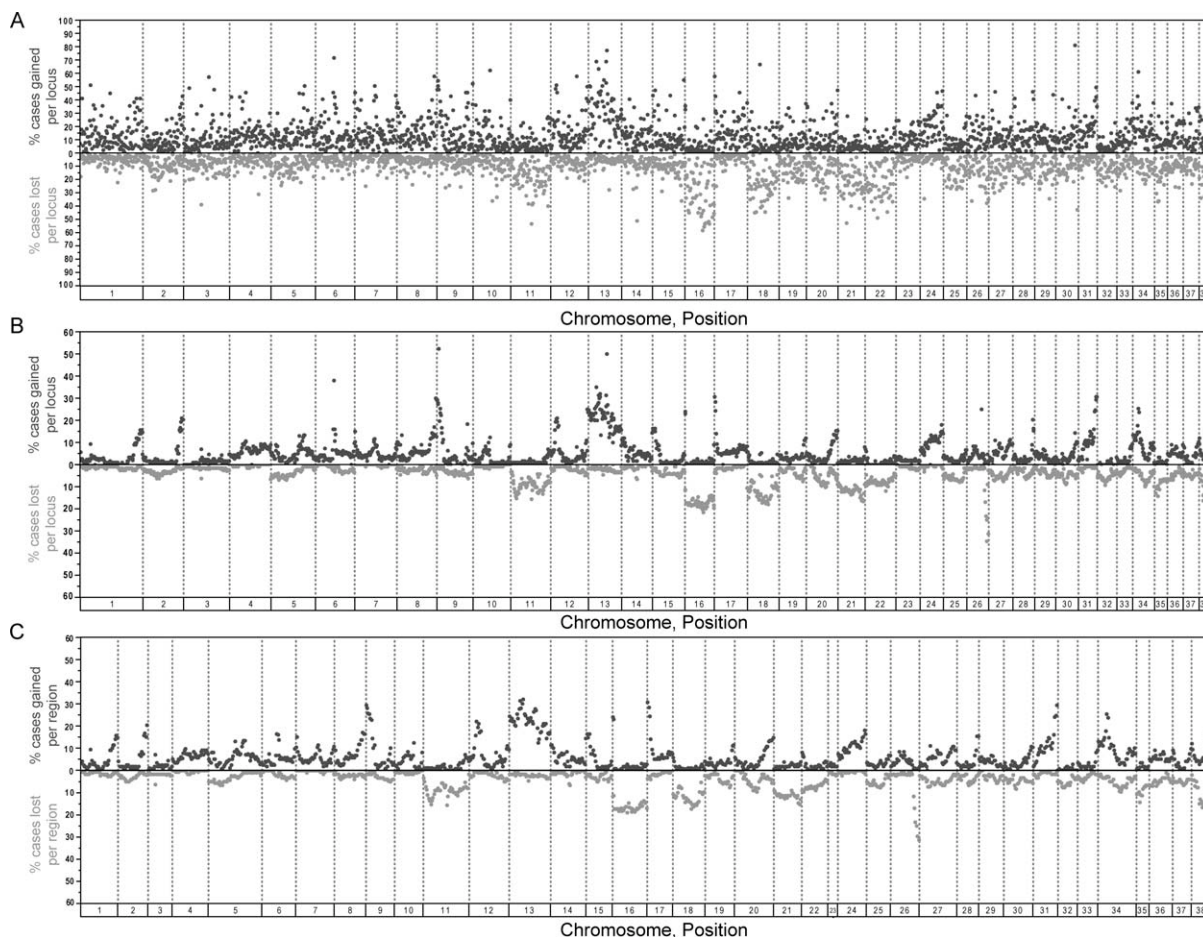
Figure 1. Frequency of copy number aberration in 123 canine OS samples. The 38 dog autosomes are listed on the x-axis. The y-axis shows the percentage of cases with copy number gain (dark grey dots) and copy number loss (light grey dots), for each ~ 1 Mb interval, based on log₂ ratios before and after data processing by the aCGH Smooth algorithm (Jong et al., 2003). A: Graphical representation of the aberration percentages across 123 canine OS patients based on the raw log₂ ratio values for chromosomal loci. B: Data in A after being processed with the aCGH Smooth algorithm (Jong et al., 2003). C: Graphical representation of aberration percentages in B, now for 1,066 regions of collapsed data, based on aberration commonality. Regions of CNAs were collapsed according to inflection points of copy number gain, loss, or normality across 123 canine OS patients, which caused the chromosomal size and distribution differences between A, B, (spaced at 1 Mb intervals) and C (which is spaced according to the number of recurrent aberration regions present within each chromosome).

from numerous single locus CNAs to whole chromosome aneuploidy. FISH data provided evidence for frequent structural changes also. The extent of the genomic imbalances across the cohort is represented in Figure 1, which denotes the percentages of gains and losses at ~ 1 Mb intervals across all 38 canine autosomes based on log₂ ratios before and after data processing by the aCGH Smooth algorithm (Jong et al., 2003) (Figs. 1A and 1B). Prior to the data being processed by the aCGH Smooth algorithm (Fig. 1A), each arrayed locus exhibited some frequency of copy number gain and/or loss, reiterating the chaotic nature of the disease. Application of the aCGH Smooth algorithm exposed the most prominent genomic regions containing CNAs within our ca-

nine OS dataset. Analysis of the 123 cases for inflection points (change in copy number status) separating regions of chromosomal gain, loss, or normal copy number across cases, collapsed the data into 1,066 larger regions of recurrent contiguous copy number status (Fig. 1C). The large number of shared regional aberrations indicates the broad positional range of gain/loss in each OS patient. The distribution shift across the autosomes shows the degree of disease complexity per chromosome and the variance of genomic aberrations between patients (Figs. 1B and 1C). Subsequent data analysis was based on comparison between aberration frequencies within these 1,066 regions of the genome. As shown in Figure 2A the majority of the aberration regions
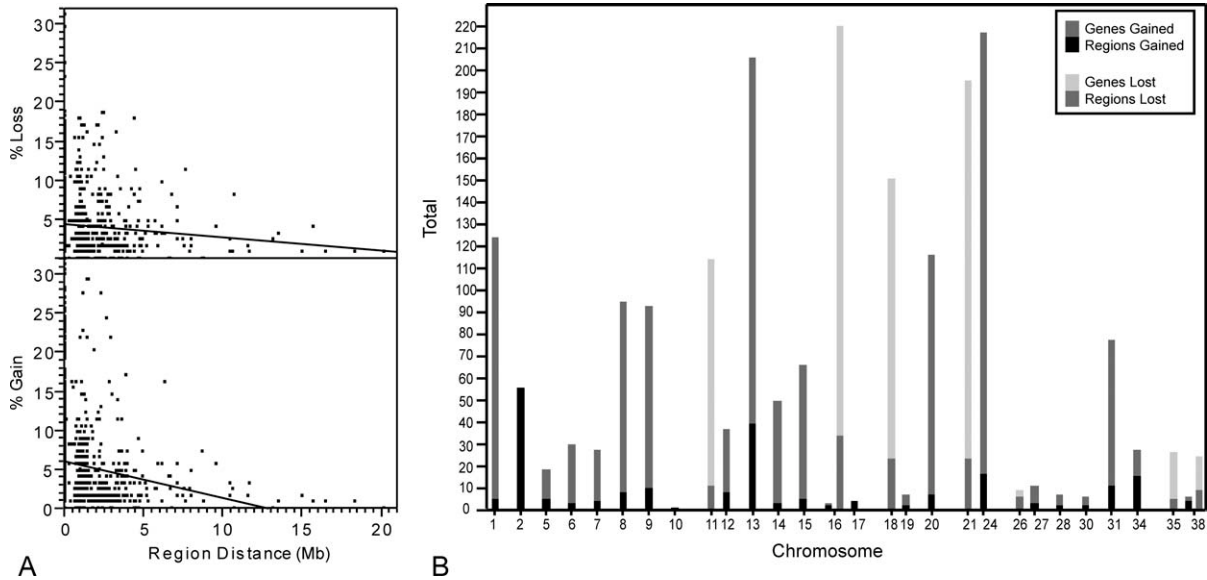
Figure 2. A: Bivariate fit of CNA percent loss/gain for 123 canine OS cases by the physical size of the aberrations in Mb. B: Total number of recurrent aberration regions (>10%) in our dog OS cohort and the total number of mapped human refseq genes within these regions using the UCSC genome browser (http://genome.ucsc.edu) separated by dog chromosome.

in our canine OS dataset were individual, occurring in <10% of the cohort. Thus, to conduct further biological investigation of high frequency aberration regions in our cohort using the Database for Annotation, Visualization, and Integrated Discovery (DAVID) v6.7 for functional annotation analysis (http://david.abcc.ncifcrf.gov/), we set the level of 'recurrent' copy number aberrations at >10% of the cohort. This captured 15% of the regions exhibiting copy number gain and 10% of regions exhibiting copy number loss. Within the sample population seven chromosomes contained regions that had >10% copy number loss, while 23 chromosomes had regions with a frequency of copy number gain >10%. Dog chromosome 23 (CFA 23) appeared to be the least aberrant chromosome with little variation between patients. As seen in Figure 1C and Supporting Information Figure 3, 46 loci (spaced at ∼ 1 Mb intervals) on CFA 23 could be segmented into just nine regions, with no regional aberration frequency >4%. The majority of regions experiencing an aberration (gain or loss) frequency greater than 10% were <5 Mb in size, while regions with <5% aberration frequency were generally larger in size (Fig. 2A). Linear regression analysis indicated that the association of high aberration frequency with smaller aberration size was statistically significant for regions

experiencing both gain ($P = 1.549e^{-8}$) and/or loss ($P = 0.00987$).

Identification of recurrent genomic aberrations in the 1,066 regions allowed further characterization of CNAs and were consistent with our previous findings (Thomas et al., 2009b). To obtain full gene annotation coverage all human refseq genes that map to orthologous dog genomic recurrent aberration regions with >10% frequency of gain and loss in our cohort were identified using the UCSC table genome browser (Fig. 2B, Supporting Information Tables 3 and 4). Twenty of the 23 chromosomes that had a high frequency of copy number gain (>10%) contained orthologous gene annotation and all seven chromosomes with high copy number loss contained gene annotation. Chromosome 13 contained the highest number of recurrent copy number gain regions, whereas chromosome 16 contained the highest number of recurrent regions of copy number loss (Fig. 2B, Supporting Information Tables 3 and 4). These gene lists were submitted to DAVID for functional annotation analysis (http://david.abcc.ncifcrf.gov/). For subsequent FISH and qRT-PCR analyses, we assessed the gene list provided by DAVID and compared this with genes reported in previous studies of human and canine OS. Based on the availability of cases in our cohort for which all of
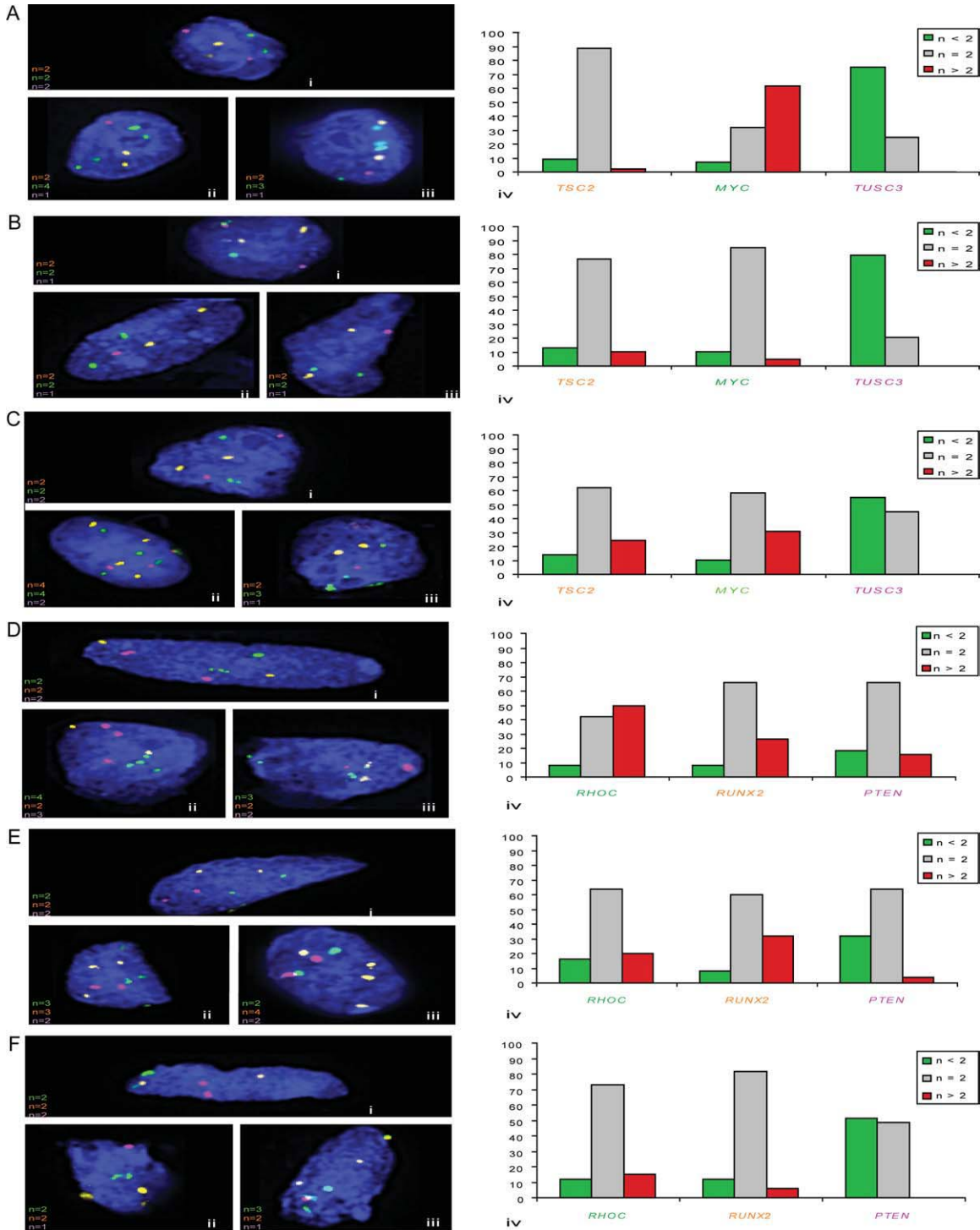
Figure 3. Interphase multicolor FISH analysis of three zinc fixed paraffin embedded canine OS tissues using BAC clone probe sets encompassing three genes (*TSC2*, *MYC*, and *TUSC3*) and (*RUNX2*, *RHOC*, and *PTEN*) (Supporting Information Table 2). *TSC2* and *RUNX2* are represented by the orange signal, *MYC* and *RHOC* by the green signal, and *TUSC3* and *PTEN* by the pink signal. In each graph the x-axis represents the gene and the y-axis demonstrates the percentages of nuclei for the stated copy number of each clone. A, B, C, D, E, and F show FISH analysis of four cases: A = 10-yr-old male Rottweiler with osteoblastic OS, B, D = 12-yr-old female Great Pyrenees with chondroblastic OS, C, F = 6-yr-old female retired racing Greyhound with OS, E = 6-yr-old female Golden Retriever with osteoblastic OS. For each case data are shown as: (i) interphase nucleus of a cell from each case presenting with a normal copy number (n = 2) of each of the three genes being assessed; (ii, iii) abnormal interphase nucleus from each patient demonstrating the presence of an aberrant copy number (n ≠ 2) for one or more of *TSC2*, *MYC*, and *TUSC3* or *RUNX2*, *RHOC*, and *PTEN*. (iv) Compilation of copy number data of the set of three genes assessed for each case, based on FISH analysis.

tumor DNA, RNA, and cells were available, we identified four genes (*TSC2*, *RHOC*, *RUNX2*, and *MYC*) in regions of recurrent copy number gain and two genes (*TUSC3*, *PTEN*) in regions of recurrent high copy number loss for subsequent evaluation. *TSC2* and *MYC* are oncogenes, *RHOC* is involved in signal tranduction pathways, *RUNX2* is involved in osteoblast differentiation, and *TUSC3* and *PTEN* are tumor suppressor genes.

FISH Validation of aCGH Data

Interphase and metaphase multicolor FISH analyses were conducted to validate specific CNAs indicated by aCGH using BAC clones selected from within six regions of the genome identified as recurrently aberrant in our cohort of OS patients, and which also contained genes of possible interest: *TSC2*, *RHOC*, *RUNX2*, *MYC*, *TUCS3*, and *PTEN* (Supporting Information Tables 2, 3, and 4). Cells from 18 FFPE canine OS specimens (highlighted in Supporting Information Table 1) were evaluated by interphase FISH. Analysis of FFPE derived cells from four of the eighteen cases is shown in Figure 3, demonstrating the typical degree of numerical aberration present in the cases evaluated in this study. For each case evaluated the copy number evident using FISH analysis supported the aCGH data and the high degree of tumor heterogeneity in canine OS. To demonstrate the extent of both numerical and structural aberration, metaphase FISH analysis of regions of CFA 13 in canine OS is shown in Supporting Information Figure 3. The two BAC clones selected from within the region of copy number increase were both present as >eight copies in this case, along with structural rearrangements of CFA 13 (Supporting Information Fig. 3B).

Breed and Morphological Subtype Specific Associated DNA Copy Number Aberrations

The variation in frequency of the 1,066 regions of recurrent aberration between the five major breeds groups and three morphological OS subtypes are indicated in Figure 4. A Fisher's exact test revealed no significant difference (after applying a multiple testing correction) between aCGH-defined regional aberrations and breed groups, when comparing results between all five breed groups together and individually. The region CFA

15q12 (10.64-10.84 Mb), was trending towards a different aberration frequency between the five groups (uncorrected $P = 0.00242$) (Fig. 4A). Forty four percent (11/25 cases) of Greyhounds had a high frequency of DNA copy number gain in this region of CFA 15, whereas in the other breed groups the frequency of gain was greatly reduced: Great Pyrenees (0%; 0/13 cases), Golden Retriever (4.5%; 1/22 cases), Rottweiler (17.6%; 6/34 cases), and non-target/other breeds (6.9%; 2/29 cases). The Fisher's exact test comparing the aCGH aberration results for patients with osteoblastic or chondroblastic OS identified a significant difference (Bonferroni corrected $P < 0.05$) in two consecutive regions of CFA 5q11-q12 (3.14–7.02 Mb and 8.01–9.26 Mb). Of the 12 chondroblastic OS patients, four (33%) demonstrated copy number gain in both these two regions, whereas none of the 67 osteoblastic patients displayed copy number gain of these regions (Fig. 4B).

qRT-PCR

To assess the correspondence of DNA copy number changes present in canine OS with an increase or decrease in expression, we analyzed the same six genes evaluated by FISH analysis by qRT-PCR. We compared expression levels in OS to those present in RNA isolated from nonneoplastic femur from an adult mixed breed dog. High quality RNA was available for 26 of the 123 cases assessed by aCGH and so these were used for qRT-PCR. Evaluation of this group of 26 canine OS cases indicated that four of the six genes investigated (*PTEN*, *RHOC*, *RUNX2* and *TUSC3*) showed recurrent expression changes (>2 fold change) that were in agreement with the corresponding genomic DNA CNA revealed by aCGH (Fig. 5). For *MYC* and *TSC2*, while the BACs on our 1 Mb array containing these loci both had recurrent copy number gain (25.2% and 16.3%), we did not see any changes in expression levels of these two genes. qRT-PCR data indicated that *RHOC* and *RUNX2* were overexpressed and *PTEN* and *TUSC3* were under-expressed in our canine OS patients. Although *RHOC* was overexpressed, it did not show a significant association between mean fold change and CNA when using a nonparametric Kruskal-Wallis test ($P = 0.4715$). Loss of *PTEN* expression is consistent with previous research (Levine et al., 2002) on canine OS, and unlike *RHOC* we did find a statistically significant association between the mean fold change for cases that exhibited either a normal or
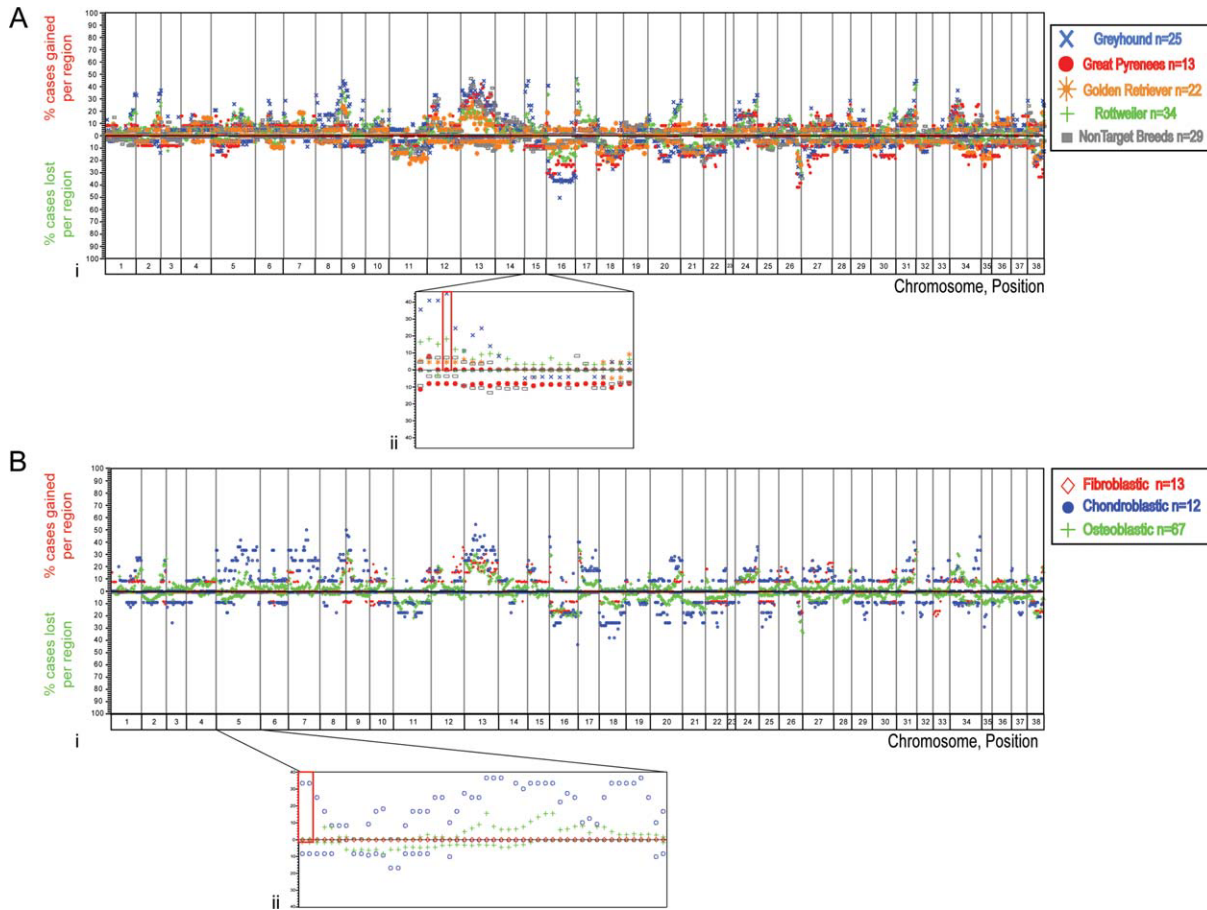
Figure 4. Further characterization of copy number aberration occurrences across 1,066 regions of aberration commonality in the 38 dog autosomes (*x*-axis). Percentages of copy number gain/loss are shown on the *y*-axis (A). Percentage CNA in different dog breeds represented within our 123 case dataset (i) with an enlarged view of the region trending towards a different aberration frequency between the five breed groups, CFA 15q12 (10.62–10.84 Mb), marked by a red box (ii). The 'non-target' breed group is a combination of 29 dogs representing 15 breeds, each with fewer than five cases (Table 1). (B) Percentage of CNA present in the 93 (of 123) cases within the study that were defined according to histomorphological subtype: fibroblastic, chondroblastic, and osteoblastic (i) with an enlarged view of the regions with a significant difference in aberration frequency between osteoblastic and chondroblastic OS cases, CFA 5q11-q12 (3.14–7.02 MB and 8.01–9.26 Mb), marked by a red box (ii).

loss of copy number using a nonparametric Kruskal-Wallis test ($P = 0.0158$). In addition, *RUNX2* ($P = 0.0077$) and *TUSC3* ($P = 0.0449$) displayed a statistically significant association between mean fold change and CNA suggesting that CNAs for these particular genes does affect the expression level. Using a Cox Proportional Hazard test, expression changes in these patients were not identified as having a significant effect on their survival time. This is because treatment still remains the driving factor affecting patient outcome ($P = 0.0016$) (Supporting Information Fig. 1).

DISCUSSION

In human OS the complex karyotypes (Papachristou and Papavassiliou, 2007; Clark et al., 2008; Tang et al., 2008) and rarity of the disease have confounded the ability to define specific genetic changes that ultimately lead to the disease phenotype. Knowledge gained from analysis of model organisms is thus important to advancing genomic characterization of these cancers. Spontaneous OS is not a rare disease in the domestic dog, with reported annual cases being at least tenfold higher than in humans, yet very few studies have profiled the disease for its genomic instability. In previous preliminary studies, using low resolution CGH, we reported that dogs ($n = 38$) with OS have a broad range of numerical and structural cytogenetic aberrations, suggesting that the disease in dogs and humans presents with similarly high levels of genome wide CNA (Thomas et al., 2009b). In the present study, we profiled 123 canine OS cases from four key breeds and of three
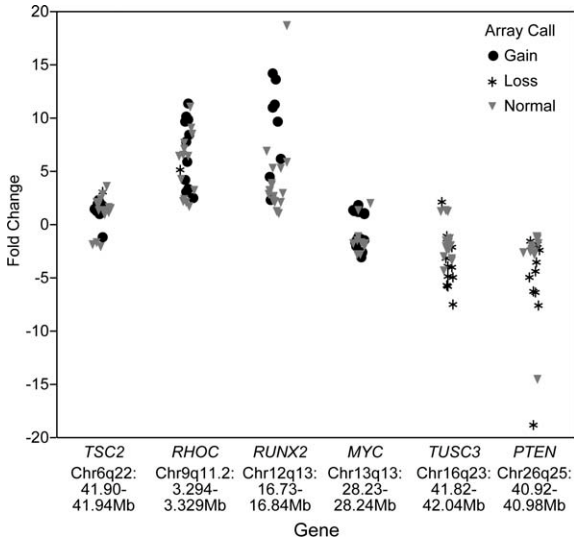
Figure 5. Quantitative RT-PCR on 26 canine OS patients for six genes located in regions that experienced a high occurrence of CNAs. The results are displayed as fold change in expression relative to non-neoplastic dog femur RNA normalized by the expression of *c12orf43*. The symbol of the marker refers to the array CGH call (gain, loss, or normal) of each OS case.

major histomorphologic cell types, at a tenfold higher resolution, to further characterize the genomic imbalance found in dog OS. These data indicate that canine OS presents with extensive genomic imbalance, with CNAs more likely to involve subchromosomal regions than entire chromosomes and with genomic interval size of CNAs significantly associated with their frequency in an inverse relationship (Fig. 2A). In most cases, the aCGH profiles were not segmented into discrete regions with narrow ranges of $\log_2$ values, indicative of a high level of CNA heterogeneity within the tumor cell population. This is a feature shared with aCGH profiles of human OS, as is the higher incidence of DNA copy number gain over DNA copy number loss (Man et al., 2004; Selvarajah et al., 2008). In addition, we analyzed several target genes in regions of genomic instability by qRT-PCR to determine if alteration to gene dosage corresponded with transcriptional dysregulation. Thus, we have concluded that orthologous genomic regions of humans and dogs have some of the same types of CNAs in OS as well as similar expression patterns.

In human OS, high-level amplifications have been reported in 8q21-24 (Man et al., 2004; Selvarajah et al., 2008; Sadikovic et al., 2009). This region is orthologous to CFA 13q12.3-q13, which was within the region exhibiting the highest frequency of copy number gain (>20% for all regions) in our canine OS cohort (Figs. 1 and 2B,

Supporting Information Table 3). Our FISH data demonstrated that CNAs of CFA 13 were associated also with structural alterations in the OS genome (Supporting Information Fig. 2). Numerous genes map within the conserved region defined by HSA 8q21-24/CFA 13q13.3-q13 (Supporting Information Table 3), several of which already have been associated with known cancer phenotypes, cell growth, and intracellular signal transduction pathways, including *ENPP2*, *MYC*, and *PSCA*, (Tang et al., 2008; Jonkers and Moolenaar, 2009; Wu et al., 2009). Seven to twelve percent of human OS have amplifications of the *MYC* oncogene (Tang et al., 2008) and copy number gains of *MYC* have been confirmed previously in canine OS (Thomas et al., 2009b). Within our cohort FISH analysis of *MYC* also demonstrated copy number gains of the oncogene (Fig. 3) and our expression analysis of *MYC* concluded that although the gene is subject to recurrent gene dosage increase in our canine OS cohort it does not appear to produce a corresponding increase in expression levels (Fig. 5). Previously, overexpression of *MYC* has been found to play a role in human OS (Gamberi et al., 1998; de Nigris et al., 2007), yet very recently Sadikovic et al. showed that no significant changes in expression of *MYC* occurred in tumors in comparison with normal osteoblasts (Sadikovic et al., 2010). Our findings in canine OS support this recent observation. Further investigation into effects of myc protein expression would be necessary to understand the role of copy number gain of *MYC* in canine OS.

Human chromosome band 6p21.1 (40.6-45.2 Mb) has been identified as a key region of copy number gain in human OS (Selvarajah et al., 2008; Sadikovic et al., 2009). The evolutionarily conserved region in the canine genome is CFA12q13 (12.21–16.73 Mb), which was subject to copy number gain in 17% of our cohort. Within this region is the *RUNX2* gene, a member of the *RUNX* gene family of differentiation mediators expressed at different stages of osteoblast development (Ito, 2004). It has been hypothesized that the amplification and overexpression of *RUNX2* in primary human OS tumors could disrupt G2/M cell cycle checkpoints, and downstream OS-specific changes, such as genomic polyploidization and failure of bone differentiation (Sadikovic et al., 2009). When studying the functions of *RUNX2* in immortalized mouse calvarial derived MC3T3-E1 osteoblasts and rat and human OS cell lines, a high expression level of *RUNX2* in late G_1 and mitosis was reported (San Martin

et al., 2009). We conducted qRT-PCR to identify if copy number gain of *RUNX2* is associated with overexpression of the gene in canine OS. We found a statistically significant difference between cases with normal or increased copy number and changes in expression. This same pattern of increase in copy number leading to an increase in expression has been found in human OS (Sadikovic et al., 2009) making this gene valuable to study of OS in both species. Additionally, recent evaluation of 16 genes as potential biomarkers of human OS oncogenesis and chemotherapy response concluded that a significant increase in *RUNX2* expression corresponded with poor patient response to chemotherapy relative to the good responders (Sadikovic et al., 2010). These data suggest that *RUNX*, as an OS-associated gene, may be important for disease progression and is of interest for further characterization in canine OS. To our knowledge this is the first indication of the possible role of *RUNX2* in canine OS.

Regions experiencing highly recurrent (>10%) copy number loss reside largely on two chromosomes, CFA 26 and CFA 16 (Fig. 2B, Supporting Information Table 4). In human OS the *PTEN* tumor suppressor gene has a high frequency of copy number loss, often a homozygous deletion resulting in complete loss of *PTEN* expression (Freeman et al., 2008). Our current findings (Figs. 1, 2B, and 3, Supporting Information Table 4) support two previous canine studies: our own, which identified frequent deletion of *PTEN* (Thomas et al., 2009b) and a second in which *PTEN* was found mutated or downregulated in a high percentage of canine OS cell lines and tumors (Levine et al., 2002). *PTEN* was deleted at a frequency of 30% in our cohort and the qRT-PCR data revealed *PTEN* as underexpressed in several cases (Fig. 5) corresponding to a decrease in copy number. Thus our data suggest that in combination with other factors, a change in gene dosage may have an effect on the transcriptional regulation of *PTEN* in canine OS.

Another region of high copy number loss in our dataset contained the candidate tumor suppressor gene, *TUSC3*. To our knowledge, loss of *TUSC3* has not been described previously in either human or canine OS. Yet, high resolution aCGH of human breast cancer cell lines and primary tumors concluded that the copy number loss of *TUSC3* resulted in decreased expression in cell lines, and absent or reduced expression in 31% of primary breast tumors (Cooke et al., 2008). Our expression analysis indicated that *TUSC3* was under-expressed, and we found a statistically significant difference between mean RNA fold change and deletion indicating that, as with *PTEN*, copy number loss in combination with other factors may be causal in reducing gene expression. As far as we are aware, this study has been the first to consider *TUSC3* as a gene involved in canine OS. *TUSC3* is thus of interest for further study in human OS because of the high degree of similarity shared with copy number aberrations in dogs and humans.

In combination with defining genomic CNAs shared with human OS, we attempted to identify differences in CNAs between the five breed groups and three morphological subtypes represented in our sample set. No significant differences between the five breed groups were found (after a multiple testing correction). Low power, because of a limited sample size for each breed group after sample recruitment, is a potential explanation for these results and further studies are needed to fully elucidate the possible significance of this region.

In considering OS morphological subtype, we identified that for two adjacent aberrant regions of CFA 5 (3.14–7.02 Mb and 8.01–9.26 Mb) there was a significantly higher frequency of copy number gain in osteoblastic compared with chondroblastic tumors (Fig. 4B). A difference in genomic imbalance between the morphological subtypes of OS is not well established, but it was previously concluded that dogs with the osteoblastic minimally productive subtype, but not chondroblastic or telangiectatic subtypes, differed from fibroblastic OS in being associated with a significantly higher number of high-grade cases (Loukopoulos and Robinson, 2007) Although this was a small sample size and the majority of canine OS patients had osteoblastic OS, investigation of this region could serve to distinguish one subtype from another. Further characterization of their possible effect on the tumor phenotype could lead to the development of more tailored therapies based on the histological profile of the tumor.

In profiling 123 cases of canine OS by 1 Mb aCGH, we concluded that the high occurrence of genetic alterations characteristic of human OS is also a striking feature of canine OS, supporting previous canine studies (Thomas et al., 2009b). We identified several new candidate genes, including *TSC2*, *RHOC*, *RUNX2*, *MYC*, *TUSC3*, and *PTEN*, in regions of the canine genome that

had highly recurrent CNAs (Supporting Information Tables 3 and 4) and were able to categorize specific CNAs into different canine OS morphological subtypes, suggesting that disease pathogenesis may differ depending on an individual's genetic background. Further evaluation of these regions of CNAs, by molecular and immunohistochemical approaches may identify specific differences in the genetic pathways. The canine orthologous regions to HSA 6p21.1 and HSA 8q24 presented with the same pattern of CNAs in dog OS, indicative of an evolutionarily conserved genetic basis for the disease. Of specific interest is the gene *RUNX2*, which resides within the orthologous regions defined by HSA 6p21.1 and CFA 12q13. Several recent studies have focused on investigating the dysregulation of *RUNX2* in human OS (Pereira et al., 2009; Sadikovic et al., 2009, 2010; San Martin et al., 2009; Shapovalov et al., 2010), and the comparability of our data suggests that *RUNX2* merits further investigation in both species.

The discoveries reported here provide additional insight into the chaotic genome organization of a cancer that affects more than 10,000 dogs per year in the United States. This study highlights the remarkably high extent to which cytogenetic abnormalities in OS are conserved between both species, supporting the role of the dog as a valid comparative model of human OS. Analysis of selected gene expression patterns in human and canine OS indicated similarities at the transcriptional level also, further supporting the functional significance of such aberrations. Overall, these data reinforce the impact that genomic analysis of canine OS may have on pinpointing key genes in human OS and which warrant subsequent examination.

REFERENCES

Abdi H. 2007. Bonferroni and Šidák corrections for multiple comparisons. In: Salkind NJ, editor. Encyclopedia of Measurement and Statistics. Thousand Oaks, CA: Sage, pp 103–107.

Bayani J, Zielenska M, Pandita A, Al-Romaih K, Karaskova J, Harrison K, Bridge JA, Sorensen P, Thorner P, Squire JA. 2003. Spectral karyotyping identifies recurrent complex rearrangements of chromosomes 8, 17, and 20 in osteosarcomas. Genes Chromosomes Cancer 36:7–16.

Breen M, Langford CF, Carter NP, Holmes NG, Dickens HF, Thomas R, Suter N, Ryder EJ, Pope M, Binns MM. 1999. FISH mapping and identification of canine chromosomes. J Hered 90:27–30.

Breen M, Hitte C, Lorentzen TD, Thomas R, Cadieu E, Sabacan L, Scott A, Evanno G, Parker HG, Kirkness EF, Hudson R, Guyon R, Mahairas GG, Gelfenbeyn B, Fraser CM, Andre C, Galibert F, Ostrander EA. 2004. An integrated 4249 marker FISH/RH map of the canine genome. BMC Genomics 5:65.

Bridge JA, Nelson M, McComb E, McGuire MH, Rosenthal H, Vergara G, Maale GE, Spanier S, Neff JR. 1997. Cytogenetic findings in 73 osteosarcoma specimens and a review of the literature. Cancer Genet Cytogenet 95:74–87.

Clark JC, Dass CR, Choong PF. 2008. A review of clinical and molecular prognostic factors in osteosarcoma. J Cancer Res Clin Oncol 134:281–297.

Cooke SL, Pole JC, Chin SF, Ellis IO, Caldas C, Edwards PA. 2008. High-resolution array CGH clarifies events occurring on 8p in carcinogenesis. BMC Cancer 8:288.

De Maria R, Miretti S, Iussich S, Olivero M, Morello E, Bertotti A, Christensen JG, Biolatti B, Levine RA, Buracco P, Di Renzo MF. 2009. met oncogene activation qualifies spontaneous canine osteosarcoma as a suitable pre-clinical model of human osteosarcoma. J Pathol 218:399–408.

de Nigris F, Botti C, Rossiello R, Crimi E, Sica V, Napoli C. 2007. Cooperation between Myc and YY1 provides novel silencing transcriptional targets of α3β1-integrin in tumour cells. Oncogene 26:382–394.

Derrien T, Andre C, Galibert F, Hitte C. 2007. AutoGRAPH: An interactive web server for automating and visualizing comparative genome maps. Bioinformatics 23:498–499.

Feugeas O, Guriec N, Babin-Boilletot A, Marcellin L, Simon P, Babin S, Thyss A, Hofman P, Terrier P, Kalifa C, Brunat-Mentigny M, Patricot LM, Oberling F. 1996. Loss of heterozygosity of the RB gene is a poor prognostic factor in patients with osteosarcoma. J Clin Oncol 14:467–472.

Forus A, Weghuis DO, Smeets D, Fodstad O, Myklebost O, Geurts van Kessel A. 1995. Comparative genomic hybridization analysis of human sarcomas. II. Identification of novel amplicons at 6p and 17p in osteosarcomas. Genes Chromosomes Cancer 14:15–21.

Fossey SL, Liao AT, McCleese JK, Bear MD, Lin J, Li PK, Kisseberth WC, London CA. 2009. Characterization of STAT3 activation and expression in canine and human osteosarcoma. BMC Cancer 9:81.

Freeman SS, Allen SW, Ganti R, Wu J, Ma J, Su X, Neale G, Dome JS, Daw NC, Khoury JD. 2008. Copy number gains in EGFR and copy number losses in PTEN are common events in osteosarcoma tumors. Cancer 113:1453–1461.

Gamberi G, Benassi MS, Bohling T, Ragazzini P, Molendini L, Sollazzo MR, Pompetti F, Merli M, Magagnoli G, Balladelli A, Picci P. 1998. C-myc and c-fos in human osteosarcoma: Prognostic value of mRNA and protein expression. Oncology 55:556–563.

Gokgoz N, Wunder JS, Mousses S, Eskandarian S, Bell RS, Andrulis IL. 2001. Comparison of p53 mutations in patients with localized osteosarcoma and metastatic osteosarcoma. Cancer 92:2181–2189.

Huang da W, Sherman BT, Tan Q, Collins JR, Alvord WG, Roayaei J, Stephens R, Baseler MW, Lane HC, Lempicki RA. 2007. THE DAVID Gene Functional Classification Tool: a novel biological module-centric algorithm to functionally analyze large gene lists. Genome Biol 8:R183.

Ito Y. 2004. Oncogenic potential of the RUNX gene family: 'Overview'. Oncogene 23:4198–4208.

Jong K, Marchiori E, van der Vaart A, Ylstra B, Weiss M, Meijer G. 2003. Chromosomal breakpoint detection in human cancer. Appl Evol Comput 2611:54–65.

Jonkers J, Moolenaar WH. 2009. Mammary tumorigenesis through LPA receptor signaling. Cancer Cell 15:457–459.

Kirpensteijn J, Kik M, Rutteman GR, Teske E. 2002. Prognostic significance of a new histologic grading system for canine osteosarcoma. Vet Pathol 39:240–246.

Kirpensteijn J, Kik M, Teske E, Rutteman GR. 2008. TP53 gene mutations in canine osteosarcoma. Vet Surg 37:454–460.

Levine RA. 2002. Overexpression of the sis oncogene in a canine osteosarcoma cell line. Vet Pathol 39:411–412.

Levine RA, Fleischli MA. 2000. Inactivation of p53 and retinoblastoma family pathways in canine osteosarcoma cell lines. Vet Pathol 37:54–61.

Levine RA, Forest T, Smith C. 2002. Tumor suppressor PTEN is mutated in canine osteosarcoma cell lines and tumors. Vet Pathol 39:372–378.

Lim G, Karaskova J, Vukovic B, Bayani J, Beheshti B, Bernardini M, Squire JA, Zielenska M. 2004. Combined spectral karyotyping, multicolor banding, and microarray comparative genomic hybridization analysis provides a detailed characterization of complex structural chromosomal rearrangements associated with gene amplification in the osteosarcoma cell line MG-63. Cancer Genet Cytogenet 153:158–164.

Lim G, Karaskova J, Beheshti B, Vukovic B, Bayani J, Selvarajah S, Watson SK, Lam WL, Zielenska M, Squire JA. 2005. An integrated mBAND and submegabase resolution tiling set (SMRT) CGH array analysis of focal amplification, microdeletions, and ladder structures consistent with breakage-fusion-bridge cycle events in osteosarcoma. Genes Chromosomes Cancer 42:392–403.

Lindblad-Toh K, Wade CM, Mikkelsen TS, Karlsson EK, Jaffe DB, Kamal M, Clamp M, Chang JL, Kulbokas EJ, III, Zody MC, Mauceli E, Xie X, Breen M, Wayne RK, Ostrander EA, Ponting CP, Galibert F, Smith DR, DeJong PJ, Kirkness E, Alvarez P, Biagi T, Brockman W, Butler J, Chin CW, Cook A, Cuff J, Daly MJ, DeCaprio D, Gnerre S, Grabherr M, Kellis M, Kleber M, Bardeleben C, Goodstadt L, Heger A, Hitte C, Kim L, Koepfli KP, Parker HG, Pollinger JP, Searle SM, Sutter NB, Thomas R, Webber C, Baldwin J, Abebe A, Abouelleil A, Aftuck L, Ait-Zahra M, Aldredge T, Allen N, An P, Anderson S, Antoine C, Arachchi H, Aslam A, Ayotte L, Bachantsang P, Barry A, Bayul T, Benamara M, Berlin A, Bessette D, Blitshteyn B, Bloom T, Blye J, Boguslavskiy L, Bonnet C, Boukhgalter B, Brown A, Cahill P, Calixte N, Camarata J, Cheshatsang Y, Chu J, Citroen M, Collymore A, Cooke P, Dawoe T, Daza R, Decktor K, DeGray S, Dhargay N, Dooley K, Dorje P, Dorjee K, Dorris L, Duffey N, Dupes A, Egbiremolen O, Elong R, Falk J, Farina A, Faro S, Ferguson D, Ferreira P, Fisher S, FitzGerald M, Foley K, Foley C, Franke A, Friedrich D, Gage D, Garber M, Gearin G, Giannoukos G, Goode T, Goyette A, Graham J, Grandbois E, Gyaltsen K, Hafez N, Hagopian D, Hagos B, Hall J, Healy C, Hegarty R, Honan T, Horn A, Houde N, Hughes L, Hunnicutt L, Husby M, Jester B, Jones C, Kamat A, Kanga B, Kells C, Khazanovich D, Kieu AC, Kisner P, Kumar M, Lance K, Landers T, Lara M, Lee W, Leger JP, Lennon N, Leuper L, LeVine S, Liu J, Liu X, Lokyitsang Y, Lokyitsang T, Lui A, Macdonald J, Major J, Marabella R, Maru K, Matthews C, McDonough S, Mehta T, Meldrim J, Melnikov A, Meneus L, Mihalev A, Mihova T, Miller K, Mittelman R, Mlenga V, Mulrain L, Munson G, Navidi A, Naylor J, Nguyen T, Nguyen N, Nguyen C, Nicol R, Norbu N, Norbu C, Novod N, Nyima T, Olandt P, O'Neill B, O'Neill K, Osman S, Oyono L, Patti C, Perrin D, Phunkhang P, Pierre F, Priest M, Rachupka A, Raghuraman S, Rameau R, Ray V, Raymond C, Rege F, Rise C, Rogers J, Rogov P, Sahalie J, Settipalli S, Sharpe T, Shea T, Sheehan M, Sherpa N, Shi J, Shih D, Sloan J, Smith C, Sparrow T, Stalker J, Stange-Thomann N, Stavropoulos S, Stone C, Stone S, Sykes S, Tchuinga P, Tenzing P, Tesfaye S, Thoulutsang D, Thoulutsang Y, Topham K, Topping I, Tsamla T, Vassiliev H, Venkataraman V, Vo A, Wangchuk T, Wangdi T, Weiand M, Wilkinson J, Wilson A, Yadav S, Yang S, Yang X, Young G, Yu Q, Zainoun J, Zembek L, Zimmer A, Lander ES. 2005. Genome sequence, comparative analysis and haplotype structure of the domestic dog. Nature 438:803–819.

Loukopoulos P, Robinson WF. 2007. Clinicopathological relevance of tumour grading in canine osteosarcoma. J Comp Pathol 136:65–73.

Lu XY, Lu Y, Zhao YJ, Jaeweon K, Kang J, Xiao-Nan L, Ge G, Meyer R, Perlaky L, Hicks J, Chintagumpala M, Cai WW, Ladanyi M, Gorlick R, Lau CC, Pati D, Sheldon M, Rao PH. 2008. Cell cycle regulator gene CDC5L, a potential target for 6p12-p21 amplicon in osteosarcoma. Mol Cancer Res 6:937–946.

Man TK, Lu XY, Jaeweon K, Perlaky L, Harris CP, Shah S, Ladanyi M, Gorlick R, Lau CC, Rao PH. 2004. Genome-wide array comparative genomic hybridization analysis reveals distinct amplifications in osteosarcoma. BMC Cancer 4:45.

Mirabello L, Troisi RJ, Savage SA. 2009a. International osteosarcoma incidence patterns in children and adolescents, middle ages and elderly persons. Int J Cancer 125:229–234.

Mirabello L, Troisi RJ, Savage SA. 2009b. Osteosarcoma incidence and survival rates from 1973 to 2004: Data from the Surveillance, Epidemiology, and End Results Program. Cancer 115:1531–1543.

Overholtzer M, Rao PH, Favis R, Lu XY, Elowitz MB, Barany F, Ladanyi M, Gorlick R, Levine AJ. 2003. The presence of p53 mutations in human osteosarcomas correlates with high levels of genomic instability. Proc Natl Acad Sci U S A 100:11547–11552.

Ozaki T, Neumann T, Wai D, Schafer KL, van Valen F, Lindner N, Scheel C, Bocker W, Winkelmann W, Dockhorn-Dworniczak B, Horst J, Poremba C. 2003. Chromosomal alterations in osteosarcoma cell lines revealed by comparative genomic hybridization and multicolor karyotyping. Cancer Genet Cytogenet 140:145–152.

Paoloni M, Davis S, Lana S, Withrow S, Sangiorgi L, Picci P, Hewitt S, Triche T, Meltzer P, Khanna C. 2009. Canine tumor cross-species genomics uncovers targets linked to osteosarcoma progression. BMC Genomics 10:625.

Papachristou DJ, Papavassiliou AG. 2007. Osteosarcoma and chondrosarcoma: New signaling pathways as targets for novel therapeutic interventions. Int J Biochem Cell Biol 39:857–862.

Peduzzi P, Concato J, Kemper E, Holford TR, Feinstein AR. 1996. A simulation study of the number of events per variable in logistic regression analysis. J Clin Epidemiol 49:1373–1379.

Pereira BP, Zhou Y, Gupta A, Leong DT, Aung KZ, Ling L, Pho RW, Galindo M, Salto-Tellez M, Stein GS, Cool SM, van Wijnen AJ, Nathan SS. 2009. Runx2, p53, and pRB status as diagnostic parameters for deregulation of osteoblast growth and differentiation in a new pre-chemotherapeutic osteosarcoma cell line (OS1). J Cell Physiol 221:778–788.

Pfaffl MW. 2001. A new mathematical model for relative quantification in real-time RT-PCR. Nucleic Acids Res 29:e45.

Sadikovic B, Yoshimoto M, Chilton-MacNeill S, Thorner P, Squire JA, Zielenska M. 2009. Identification of interactive networks of gene expression associated with osteosarcoma oncogenesis by integrated molecular profiling. Hum Mol Genet 18:1962–1975.

Sadikovic B, Thorner P, Chilton-Macneill S, Martin JW, Cervigne NK, Squire J, Zielenska M. 2010. Expression analysis of genes associated with human osteosarcoma tumors shows correlation of RUNX2 overexpression with poor response to chemotherapy. BMC Cancer 10:202.

San Martin IA, Varela N, Gaete M, Villegas K, Osorio M, Tapia JC, Antonelli M, Mancilla EE, Pereira BP, Nathan SS, Lian JB, Stein JL, Stein GS, van Wijnen AJ, Galindo M. 2009. Impaired cell cycle regulation of the osteoblast-related heterodimeric transcription factor Runx2-Cbfbeta in osteosarcoma cells. J Cell Physiol 221:560–571.

Selvarajah S, Yoshimoto M, Ludkovski O, Park PC, Bayani J, Thorner P, Maire G, Squire JA, Zielenska M. 2008. Genomic signatures of chromosomal instability and osteosarcoma progression detected by high resolution array CGH and interphase FISH. Cytogenet Genome Res 122:5–15.

Shapovalov Y, Benavidez D, Zuch D, Eliseev RA. 2010. Proteasome inhibition with bortezomib suppresses growth and induces apoptosis in osteosarcoma. Int J Cancer 127:67–76.

Simons A, Janssen IM, Suijkerbuijk RF, Veth RP, Pruszczynski M, Hulsbergen-van de Kaa CA, du Manoir S, Geurts van Kessel A. 1997. Isolation of osteosarcoma-associated amplified DNA sequences using representational difference analysis. Genes Chromosomes Cancer 20:196–200.

Squire JA, Pei J, Marrano P, Beheshti B, Bayani J, Lim G, Moldovan L, Zielenska M. 2003. High-resolution mapping of amplifications and deletions in pediatric osteosarcoma by use of CGH analysis of cDNA microarrays. Genes Chromosomes Cancer 38:215–225.

Tang N, Song WX, Luo J, Haydon RC, He TC. 2008. Osteosarcoma development and stem cell differentiation. Clin Orthop Relat Res 466:2114–2130.

Tarkkanen M, Karhu R, Kallioniemi A, Elomaa I, Kivioja AH, Nevalainen J, Bohling T, Karaharju E, Hyytinen E, Knuutila S, Kallioniemi O.-P. 1995. Gains and losses of DNA sequences in osteosarcomas by comparative genomic hybridization. Cancer Res 55:1334–1338.

Tarkkanen M, Bohling T, Gamberi G, Ragazzini P, Benassi MS, Kivioja A, Kallio P, Elomaa I, Picci P, Knuutila S. 1998. Comparative genomic hybridization of low-grade central osteosarcoma. Mod Pathol 11:421–426.

Tarkkanen M, Elomaa I, Blomqvist C, Kivioja AH, Kellokumpu-Lehtinen P, Bohling T, Valle J, Knuutila S. 1999. DNA sequence copy number increase at 8q: a potential new prognostic marker in high-grade osteosarcoma. Int J Cancer 84:114–121.

Thomas R, Scott A, Langford CF, Fosmire SP, Jubala CM, Lorentzen TD, Hitte C, Karlsson EK, Kirkness E, Ostrander EA, Galibert F, Lindblad-Toh K, Modiano JF, Breen M. 2005. Construction of a 2-Mb resolution BAC microarray for CGH analysis of canine tumors. Genome Res 15:1831–1837.

Thomas R, Duke SE, Bloom SK, Breen TE, Young AC, Feiste E, Seiser EL, Tsai PC, Langford CF, Ellis P, Karlsson EK, Lindblad-Toh K, Breen M. 2007. A cytogenetically characterized, genome-anchored 10-Mb BAC set and CGH array for the domestic dog. J Hered 98:474–484.

Thomas R, Duke SE, Karlsson EK, Evans A, Ellis P, Lindblad-Toh K, Langford CF, Breen M. 2008. A genome assembly-integrated dog 1 Mb BAC microarray: A cytogenetic resource for canine cancer studies and comparative genomic analysis. Cytogenet Genome Res 122:110–121.

Thomas R, Duke SE, Wang HJ, Breen TE, Higgins RJ, Linder KE, Ellis P, Langford CF, Dickinson PJ, Olby NJ, Breen M. 2009a. 'Putting our heads together': Insights into genomic conservation between human and canine intracranial tumors. J Neurooncol 94:333–349.

Thomas R, Wang HJ, Tsai PC, Langford CF, Fosmire SP, Jubala CM, Getzy DM, Cutter GR, Modiano JF, Breen M. 2009b. Influence of genetic background on tumor karyotypes: Evidence for breed-associated cytogenetic aberrations in canine appendicular osteosarcoma. Chromosome Res 17:365–377.

Thomas R, Seiser EL, Motsinger-Reif A, Borst L, Valli VE, Kelley K, Suter SE, Argyle D, Burgess K, Bell J, Lindblad-Toh K, Modiano JF, Breen M. 2011. Refining tumor-associated aneuploidy through 'genomic recoding' of recurrent DNA copy number aberrations in 150 canine non-Hodgkin lymphomas. Leuk Lymphoma 52:1321–1335.

Tsuchiya T, Sekine K, Hinohara S, Namiki T, Nobori T, Kaneko Y. 2000. Analysis of the p16INK4, p14ARF, p15, TP53, and MDM2 genes and their prognostic implications in osteosarcoma and Ewing sarcoma. Cancer Genet Cytogenet 120:91–98.

Withrow SJ, Vail D, editors. 2007. Small Animal Clinical Oncology. Philadelphia: WB Sanders.

Withrow SJ, Powers BE, Straw RC, Wilkins RM. 1991. Comparative aspects of osteosarcoma. Dog versus man. Clin Orthop Relat Res 270:159–168.

Wu X, Ye Y, Kiemeney LA, Sulem P, Rafnar T, Matullo G, Seminara D, Yoshida T, Saeki N, Andrew AS, Dinney CP, Czerniak B, Zhang ZF, Kiltie AE, Bishop DT, Vineis P, Porru S, Buntinx F, Kellen E, Zeegers MP, Kumar R, Rudnai P, Gurzau E, Koppova K, Mayordomo JI, Sanchez M, Saez B, Lindblom A, de Verdier P, Steineck G, Mills GB, Schned A, Guarrera S, Polidoro S, Chang SC, Lin J, Chang DW, Hale KS, Majewski T, Grossman HB, Thorlacius S, Thorsteinsdottir U, Aben KK, Witjes JA, Stefansson K, Amos CI, Karagas MR, Gu J. 2009. Genetic variation in the prostate stem cell antigen gene PSCA confers susceptibility to urinary bladder cancer. Nat Genet 41:991–995.

Zhang J, Chen X, Kent MS, Rodriguez CO. 2009. Establishment of a dog model for the p53 family pathway and identification of a novel isoform of p21 cyclin-dependent kinase inhibitor. Mol Cancer Res 7:67–78.

Zielenska M, Bayani J, Pandita A, Toledo S, Marrano P, Andrade J, Petrilli A, Thorner P, Sorensen P, Squire JA. 2001. Comparative genomic hybridization analysis identifies gains of 1p35 approximately p36 and chromosome 19 in osteosarcoma. Cancer Genet Cytogenet 130:14–21.